

Growth mechanism of ZnO nanocrystals with Zn-rich from dots to rods

Guiye Shan^a, Xinli Xiao^a, Xin Wang^b, Xianggui Kong^b, Yichun Liu^{a,*}

^a Center for Advanced Optoelectronic Functional Material Research, Northeast Normal University, Changchun 130024, PR China

^b Key Laboratory of Excited States Process, Changchun Institute of Optic Fine Mechanics and Physics, Chinese Academy of Sciences, Changchun 130033, PR China

Received 1 July 2005; accepted 29 November 2005

Available online 18 January 2006

Abstract

ZnO nanocrystals from dot to rod were synthesized by simply changing Zn^{2+} concentration in ZnO seed solutions. The growth of ZnO nanocrystals was sensitive to the amount of Zn^{2+} in the solution. The growth process of ZnO from dot to rod was observed by optical spectra, transmission electron microscopy and X-ray diffraction spectra. From these results, the growth mechanism of ZnO from dots to rods was discussed. © 2005 Elsevier Inc. All rights reserved.

Keywords: ZnO; Nanorods; Growth transition; Dipole interaction

1. Introduction

Over the past decade, the rapid development of application of nanomaterials, ranging from electro-optics to biology, demands precise control their size, shape and surface properties [1–3]. Different dimensional nanomaterials could be prepared successfully at the present [4–7]. For example, size-controlled, monodisperse quantum dots were synthesized and show the properties of dependence of their electrical and optical properties on both shape and size control [8–12]. One-dimensional nanostructures, such as nanorod, nanowire, nanotube, have different synthetic routes including chemical routes (electrochemistry, template, emulsion and polymeric system) and physical routes (laser-assisted catalysis growth, vapor transport) [13–16]. These one-dimensional nanomaterials exhibit their potential technological advantages over quantum dots in many applications [17,18]. Synthesis of nanostructures via simple wet-chemical methods is one of the favored routes toward the cost-effective large-scale production of nanobuilding blocks. However, achieving control over the growth of nanostructures leading to proper dimensional confinement via wet-chemical methods is a challenging task. Introduction of templates, surface capping agents

and other physicochemical means has obtained substantial progress in controlling the size and shape of nanostructures. However, solution phase preparation of different dimensional nanostructures is still a challenging task due to surface energy and favors the formation of spherical particles. Despite the increased number of reports on the synthesis of different dimensional nanostructures in solution phase, there are few reports on the growth mechanism study of these materials from dots to rods. Understanding the formation and growth mechanism of nanomaterials from zero-dimension to one-dimension is critical for achieving control over nanoparticle properties.

In this paper, the growth process of ZnO nanocrystals was selected as a research object in solution. Based on synthesized ZnO as seeds, the growth process of ZnO nanocrystals may be obtained by injecting different amounts of Zn^{2+} . This provides a clear example of the growth transition process of different dimension nanomaterials.

2. Experimental

2.1. Chemicals

Zinc acetate ($\text{Zn}(\text{Ac})_2 \cdot 2\text{H}_2\text{O}$), lithium hydroxide ($\text{LiOH} \cdot \text{H}_2\text{O}$) were purchased from Aldrich and used as received. Ethanol (99.5%), hexane were obtained from Beijing Chemicals Corp.

* Corresponding author. Fax: +86 431 5684009.
E-mail address: ycliu@nenu.edu.cn (Y. Liu).

2.2. Preparation of ZnO seeds

The synthetic method of ZnO nanocrystals based on that of Anderson [19] with some modification. 250 ml of 0.05 M zinc acetate ethanolic solution was placed into a 500-ml three-neck round-bottom distillation flask fitted with a condenser and refluxed while stirring for 2 h at about 80 °C. The condensate was collected up to 50 ml, and 50 ml of ethanol was added into distillation flask to continuously reflux for 1 h. Then, the reaction mixture was cooled to room temperature. 0.2 M lithium hydroxide dissolved in 100 ml ethanol solution was obtained with the help of ultrasonication. Then, lithium hydroxide solution was added into the above zinc acetate solution to hydrolyze for 20 min and ZnO nanocrystals were formed. Hexane was added to ZnO solution to deposition of ZnO nanocrystals. The synthesized ZnO solution was separated by centrifugation. Finally, ZnO nanocrystals were again dispersed into ethanol solution to form 0.1 M solution.

2.3. The transition of morphologies of ZnO nanocrystals by changing the ratio of $[Zn^{2+}]/[seed]$

Appropriate quantities of ZnO seeds, LiOH, and zinc acetate solutions were taken in a test tube. 0.1 M ZnO seed solution was mixed with LiOH solution at the mole ratio of ZnO:LiOH at 1:0.5. The full mixed solution was separated into four equal parts. The zinc acetate with different mole ratio of $[Zn^{2+}]/[seed]$ from 1, 3 to 10 was respectively added to the above three solutions. Then four samples were heated and refluxed at 60 °C for 1 h. The final samples were obtained by concentration.

2.4. Instrumentation

Photoluminescence spectra were measured at room temperature with LS50 steady-state fluorescence spectrometer (Perkin–Elmer, American) on the colloidal solutions. The UV–vis spectra were measured at room temperature with a Lambda 900 UV–vis Spectrophotometer (Perkin–Elmer, American). Power X-ray diffraction (XRD) measurement was performed on Rigaku D/max-IIB X-ray Diffractometer using $CuK\alpha$ radiation (1.5406 Å) of 40 kV and 20 mA. The initial micrographs

were taken with Hitachi H-8100IV transmission electron microscope operating at 200 kV (Japan). Samples for TEM were prepared by casting one drop of the cluster solution onto a standard carbon-coated (200–300 Å) formvar film on copper grid (230 meshes). Infrared spectra were obtained on Magna 560 FTIR spectrometer with a resolution of 1 cm^{-1} .

3. Results and discussion

3.1. Effect of Zn^{2+} additives on the optical character of ZnO nanocrystals

In our experiment, our aim is to know the effect of amount of Zn^{2+} on the growth process of ZnO nanocrystals. Photoluminescence (PL) of ZnO nanocrystals including UV emission and visible emission is related to size and shape of nanocrystals. Now, we found that PL intensity of ZnO nanocrystals was sensitive to the amount of $[Zn^{2+}]$ in ZnO seed solution. As shown in Fig. 1a, PL intensity of ZnO with changing the ratio of $[Zn^{2+}]/[seed]$ has changed. Three effects are clearly visible from these spectra. First, the peaks onset of band-edge emission of ZnO nanocrystals shifts to lower energies after injecting zinc ions. The red-shift of band-edge emission position indicated that ZnO particle size increases. The absorption spectra in Fig. 1b also show the same shift. The effect can be understood in terms of a decrease in quantum confinement upon particle growth [20]. Second, the line width of band-edge emission band is gradually broadening with increasing the ratio of $[Zn^{2+}]/[seed]$, which indicated that size of ZnO particle is gradually inhomogeneous with increasing the amount of $[Zn^{2+}]$ in ZnO seed solution. Third, the intensity of UV emission corresponding to band-edge emission was enhanced while that of the visible emission decreases with increasing the amount of Zn^{2+} in ZnO seed solution. The intensity of the visible emission decreases to about half of its original value, while that of the UV emission increases by 50% with the $[Zn^{2+}]/[seed]$ ratio at 3. The visible emission disappears with the ratio of $[Zn^{2+}]/[seed]$ at 10. The visible emission of ZnO nanocrystals is related to deep-level emission. The visible emission is the transition between the electron close to the conduction band and deeply trapped hole at V_0^{**} centre (oxygen vacancy containing no electrons) [21,22]. This emission is also attributed to the transition

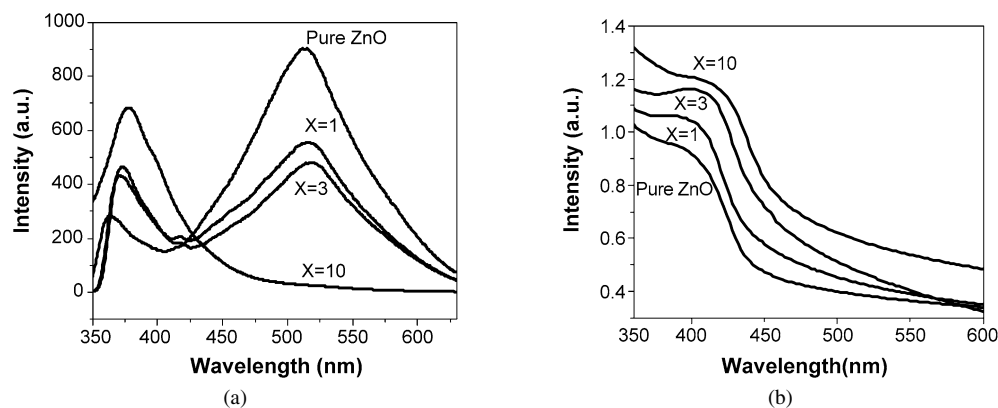


Fig. 1. Photoluminescence (a) and absorption spectra (b) of ZnO nanocrystals with different concentration of Zn^{2+} (X is corresponding to the ratio of $[Zn^{2+}]/[seed]$).

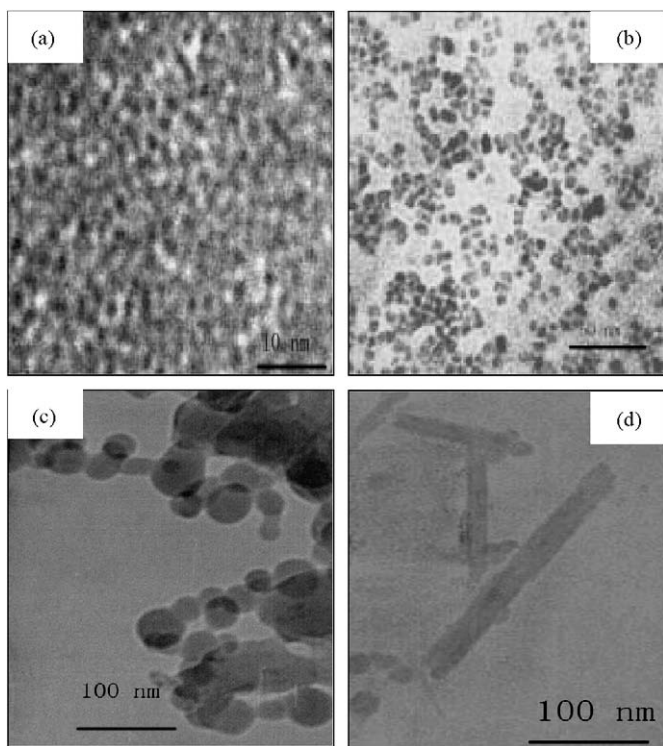


Fig. 2. Transmission electron micrographs of ZnO nanocrystals (a) and ZnO nanocrystals with $[\text{Zn}^{2+}]/[\text{seed}]$ at $x = 1$ (b), $x = 3$ (c) and $x = 10$ (d).

between the electron at $[V_0^*$ electron] or $[V_0^{**}$, two electrons] and the hole at vacancy associated with the surface defects [23]. All these evidences show that the visible emission is associated with the oxygen vacancy on the surface of ZnO nanocrystals. Electron–hole recombination at a defect site results in a large reorganization in the local charge distribution. The enhancement of band-edge emission should be due to the decrease of surface atom ratio of ZnO nanocrystals.

3.2. The morphologies and structure change of ZnO nanocrystals with Changing the Ratio of $[\text{Zn}^{2+}]/[\text{seed}]$

To learn more about the effect of the $[\text{Zn}^{2+}]/[\text{seed}]$ ratio on the morphologies of ZnO nanocrystals, transmission electron microscopy (TEM) images were obtained from the samples with different $[\text{Zn}^{2+}]/[\text{seed}]$ ratio from 0 to 10 as shown in Fig. 2. Fig. 2a shows the images of pure ZnO nanocrystals. Pure ZnO nanocrystals are dot-shapes and the sizes are about 3 nm. Figs. 2b and 2c respectively correspond to ZnO nanocrystals with $[\text{Zn}^{2+}]/[\text{seed}]$ ratio of 1 and 3. Compared to pure ZnO nanocrystals, the size of ZnO nanocrystals by injecting Zn^{2+} increases from 3 to 30 nm. The size distribution of ZnO nanocrystals with $[\text{Zn}^{2+}]/[\text{seed}]$ ratio of 1 is homogeneous and disperse. However, ZnO nanocrystals with $[\text{Zn}^{2+}]/[\text{seed}]$ ratio of 3 were aggregated to form pearl-chain-like structures. Furthermore, ZnO nanorods were formed by fusion of particles after injecting Zn^{2+} with the $[\text{Zn}^{2+}]/[\text{seed}]$ ratio of 10. The observation of TEM images is corresponding to the results of the change of PL.

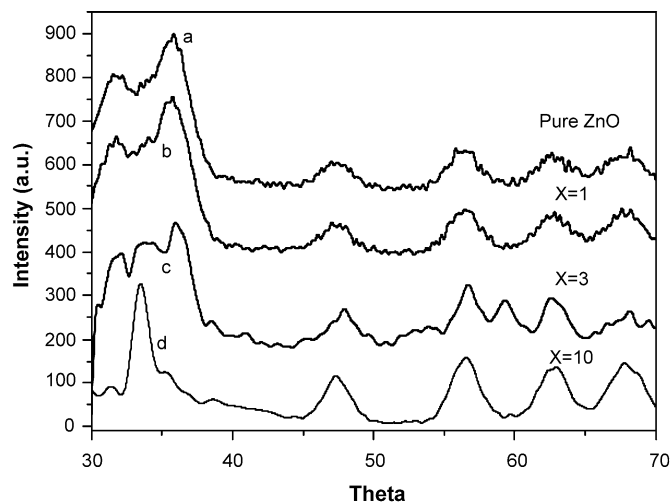


Fig. 3. XRD spectra of ZnO nanocrystals (a) and ZnO nanocrystals with $x = 1$ (b), $x = 3$ (c) and $x = 10$ (d).

To confirm the growth orientation, X-ray diffraction (XRD) spectra corresponding to samples of pure ZnO, ZnO with the $[\text{Zn}^{2+}]/[\text{seed}]$ ratio of 3 and 10 are depicted in Fig. 3. In the corresponding XRD image, the 002 reflection has strongly sharpened up which is consistent with rod formation along the c axis.

To further compare the domain sizes along different crystal orientation, we used Sherrer equation to calculate the average sizes:

$$D = \lambda / B \cos \theta,$$

where D is the average grain size, λ the X-ray wavelength, B the integral width of the peak and θ the Bragg angle.

The size of ZnO nanorods grown along (002) orientation is about 84 nm in the calculation of Sherrer equation, which is in the region of size of ZnO nanorods obtained from TEM image.

For different shapes of ZnO nanocrystals corresponding to TEM images above, infrared spectra show different stretching modes of different groups, as shown in Fig. 4. In general, ZnO nanocrystals synthesized were covered with acetate and hydroxyl pointed out by Anderson et al. In our results, hydroxyl groups and C=O groups are observed at high frequency respectively at 3350 and 1400–1500 cm^{-1} regions, as shown in Fig. 4a. Simultaneously, the stretching mode of ZnO nanocrystals may also be detected at the bands of 440 and 500 cm^{-1} , which correspond to the vibration of Zn–O [24]. The vibration peak of Zn–O of ZnO nanocrystals from dots (b), (c) to rods (d) occurred greatly by splitting. It is well known that the polarity of nanodot is weaker than that of nanorod. Thus, this great splitting indicated that the stretching polarity of Zn–O increased.

3.3. The possible growth mechanism on ZnO nanocrystals from dot to rod

ZnO nanoparticles were prepared from zinc acetate dehydrate in alcoholic solution under basic conditions. The obtained ZnO nanocrystals were used as seeds to continue to grow different dimensional nanostructures by changing zinc precursors. The procedure we have used here for making ZnO nanorods is

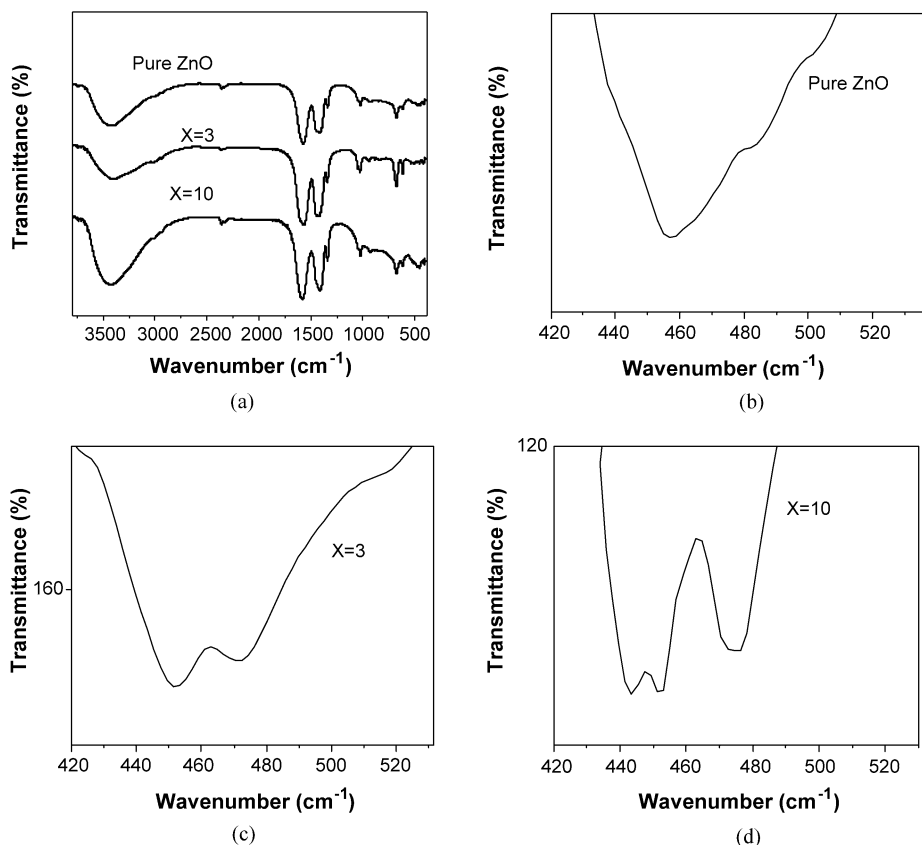


Fig. 4. IR spectra of ZnO nanocrystals and ZnO nanocrystals with different amounts of Zn(AC)₂ (a); IR characteristic peak of ZnO lies in region of 400–500 cm⁻¹. (b), (c) and (d) show the IR characteristic peak of ZnO and ZnO with $x = 3$, $x = 10$.

different from the traditional preparation procedure. Traditionally, ZnO nanorods were obtained by solvothermal, template, polymeric method [13–15]. In our experiment, we demonstrated that the growth of ZnO from dots to rods may be controlled only by the variations in $[Zn^{2+}]/[seed]$ ratio. At low $[Zn^{2+}]/[seed]$ ratio with low concentration of zinc ions, quasi-spherical particles were formed, whereas ZnO nanorods were formed at high $[Zn^{2+}]/[seed]$ ratio with high concentration of zinc ions. To learn the growth mechanism of ZnO from dot to rod, the growth procedure of ZnO nanocrystals is as following.

A typical temporal shape evolution of ZnO nanocrystals occurs in three distinguishable stages. Firstly, at low Zn ions concentration, excess OH⁻ ions in seed solution were reactive with Zn²⁺ to form ZnO clusters. The formed ZnO clusters heterogeneously grow on the surface of ZnO nanocrystals as nucleation centre. During this course, the smaller nanocrystals in the solution shrink and the bigger ones continue their growth. As a result, the size of ZnO nanocrystals was increased, but crystals grew simultaneously in three dimensions and obtained ZnO nanocrystals were quasi-spherical, as shown in Fig. 2b. This course is known as Ostwald ripening (interparticle ripening) [25]. Corresponding to Fig. 4b, the stretching peak of Zn–O is not splitting.

The second stage of the growth of ZnO nanocrystals occurs with increasing the amount of Zn precursor with the Zn²⁺/ZnO ratio of 3. In this stage, ZnO nanocrystals grew simultaneously in three dimensions. The aspect ratio remained constant, but the

crystals volume increased. Henceforth, the ZnO nanocrystals still were quasi-spherical. However, permanent dipole moment in nanocrystals has been enhanced with increasing the volume of ZnO nanocrystals. The facets terminated by negatively charged O atoms and positively charged Zn atoms have been reported by Wang [26]. As shown in Fig. 2c, the ZnO nanocrystals were connected as pearl-chain-like structures.

In the final stage of the process, as shown in Fig. 2d, all the nanocrystals grew almost exclusively along their long axis and both aspect ratio and volume of crystals increased rapidly with increasing the amount of Zn²⁺ in solution. Henceforth, ZnO nanorods were formed. The formation of ZnO nanorods furthermore increased the polarity between particles so that the infrared spectra of ZnO from dots to rods occurs greatly by splitting.

Otherwise, the surface atom ratio was decreased with increasing the volume of nanocrystals, which leads to the enhancement of photoluminescence due to the decrease of surface defects.

4. Conclusion

The secondary growth mechanism of ZnO was studied in ZnO ethanol solution with excess LiOH by injection of different amounts of zinc acetate. The $[Zn^{2+}]/[seed]$ ratio determined different growth processes of ZnO particles. At low zinc acetate concentration, the growth of ZnO was based on Ostwald

ripening process and formed ZnO particles are quasi-spherical. At intermediate concentration, oriented growth occurred among ZnO particles due to the dipole–dipole interaction and the particles were oriented-aggregated. Furthermore, at high concentration of new formed ZnO cluster, the oriented aggregation of ZnO particles was fused to form ZnO nanorod. The ZnO growth process provides a model to study the growth mechanism of nanoparticles.

Acknowledgments

This work was supported by the National Natural Science Foundation of China, (No. 60376003) and Science Foundation for Yong Teachers of Northeast Normal University (20050206).

References

- [1] V.F. Puentes, K.M. Krishnan, A.P. Alivisatos, *Science* 291 (2001) 291.
- [2] A.P. Alivisatos, *Science* 271 (1996) 933.
- [3] A.M. Morales, C.M. Lieber, *Science* 279 (1998) 208.
- [4] H.M. Cheng, J.M. Ma, L.M. Qi, *J. Am. Chem. Soc.* 125 (2003) 3450.
- [5] Z.A. Peng, X.G. Peng, *J. Am. Chem. Soc.* 123 (2001) 183.
- [6] X.H. Zhang, S.Y. Xie, Zh.Y. Jiang, *J. Phys. Chem. B* 107 (2003) 10114.
- [7] M. Yin, Y. Gu, I.L. Kuskovsky, *J. Am. Chem. Soc.* 126 (2004) 6206.
- [8] Z.A. Peng, X.G. Peng, *J. Am. Chem. Soc.* 124 (2002) 3343.
- [9] G.N. Karanikolos, P.A. Alexandridis, *Langmuir* 20 (2004) 550.
- [10] X.C. Wu, A.M. Bittner, K. Kern, *J. Phys. Chem. B* 109 (2005) 230.
- [11] C.B. Murray, D.J. Norris, M.G. Bawendi, *J. Am. Chem. Soc.* 115 (1993) 87.
- [12] N. Gaponik, D.V. Talapin, A.L. Rogach, *J. Phys. Chem. B* 106 (2002) 7177.
- [13] Y. Zhou, S.H. Yu, X.P. Cui, C.Y. Wang, Z.Y. Chen, *Chem. Mater.* 11 (1999) 545.
- [14] C.R. Martin, *Science* 226 (1994) 1961.
- [15] S. Bahattacharyya, S.K. Saha, D. Chakravorty, *Appl. Phys. Lett.* 76 (2000) 3896.
- [16] S. Iijima, *Nature* 354 (1991) 56.
- [17] A.M. Morales, C.M. Lieber, *Science* 279 (1998) 208.
- [18] T.T. Trentler, K.M. Hickman, S.C. Goel, A.M. Viano, P.C. Gibbons, W.E. Buhro, *Science* 270 (1995) 1791.
- [19] S. Sakohara, M. Ishida, M.A. Anderson, *J. Phys. Chem. B* 102 (1998) 10169.
- [20] N.S. Pesika, K.J. Stebe, P.C. Searson, *Adv. Mater.* 15 (2003) 1289.
- [21] A.V. Dijken, E. Meulenkaamp, D. Vanmaekelbergh, A. Meijerink, *J. Phys. Chem. B* 104 (2000) 1715.
- [22] A. Wood, M. Giersig, M. Hilgendorff, A.V. Campos, L.M. Lizmarzan, *Aust. J. Chem.* 56 (2003) 1051.
- [23] Y.C. Liu, X.T. Zhang, J.Y. Zhang, Y.M. Lu, X.G. Kong, D.Z. Shen, X.W. Fan, *Chin. J. Lumin.* 23 (2002) 563.
- [24] S.C. Liufu, H.N. Xiao, Y.P. Li, *Polym. Degrad. Stab.* 87 (2005) 103.
- [25] L.C. Brian, L.K. Vladimir, J.O. Charles, *Chem. Rev.* 104 (2004) 3893.
- [26] Y. Rusen, D. Yong, W. Zhonglin, *Nano Lett.* 4 (2004) 1309.